



HAL
open science

Global sensitivity analysis for the boundary control of an open channel

Alexandre Janon, Maëlle Nodet, Christophe Prieur, Clémentine Prieur

► **To cite this version:**

Alexandre Janon, Maëlle Nodet, Christophe Prieur, Clémentine Prieur. Global sensitivity analysis for the boundary control of an open channel. *Mathematics of Control, Signals, and Systems*, 2016, 28 (1), pp.6:1-27. 10.1007/s00498-015-0151-4 . hal-01065886v2

HAL Id: hal-01065886

<https://hal.science/hal-01065886v2>

Submitted on 18 Dec 2015

HAL is a multi-disciplinary open access archive for the deposit and dissemination of scientific research documents, whether they are published or not. The documents may come from teaching and research institutions in France or abroad, or from public or private research centers.

L'archive ouverte pluridisciplinaire **HAL**, est destinée au dépôt et à la diffusion de documents scientifiques de niveau recherche, publiés ou non, émanant des établissements d'enseignement et de recherche français ou étrangers, des laboratoires publics ou privés.

Global sensitivity analysis for the boundary control of an open channel

Alexandre Janon, Maëlle Nodet,
Christophe Prieur and Clémentine Prieur

the date of receipt and acceptance should be inserted later

Abstract The goal of this paper is to solve the global sensitivity analysis for a particular control problem. More precisely, the boundary control problem of an open-water channel is considered, where the boundary conditions are defined by the position of a down stream overflow gate and an upper stream underflow gate. The dynamics of the water depth and of the water velocity are described by the Shallow Water equations, taking into account the bottom and friction slopes. Since some physical parameters are unknown, a stabilizing boundary control is first computed for their nominal values, and then a sensitivity analysis is performed to measure the impact of the uncertainty in the parameters on a given *to-be-controlled output*. The unknown physical parameters are described by some probability distribution functions. Numerical simulations are performed to measure the first-order and total sensitivity indices.

1 Introduction

In this work we consider the boundary stabilization of an open channel. The model we consider is described by the Shallow-Water equations, which are conservation laws perturbed by non-homogeneous terms due to the effects of the bottom slope, the slope's friction, and the lateral supply. The boundary actions are defined as the position of both spillways located at the extremities of the reach. In [8, 14], the authors designed stabilizing boundary output feedback controllers, with an exponential convergence to the equilibrium of water level and water flow. Our interest is motivated by the following remark: in a given real open channel, many of the involved parameters are uncertain, e.g., because of measurement uncertainties (bottom slope, friction slope, ...). Our

Alexandre Janon is with Department of Mathematics, Université Paris-Sud, Orsay, France. Alexandre.Janon@math.u-psud.fr, Maëlle Nodet and Clémentine Prieur are with Université Grenoble Alpes, CNRS, and INRIA, Grenoble, France. maelle.nodet@inria.fr, clementine.prieur@imag.fr, Christophe Prieur is with Gipsa-lab, CNRS, Grenoble, France. christophe.prieur@gipsa-lab.fr

aim is then to study the sensitivity of the efficiency of the control of the open channel with respect to the uncertainties in these parameters.

This problem is related to the insensitizing problem, which consists in finding a control function such that some functional of the state is locally insensitive to the perturbations of one given parameter (usually the initial condition in the literature). For the semilinear heat equation, we can mention [5] for bounded domain and [11] for unbounded domain (see also [13] for a complete insensitization). Other works include [12] for insensitizing controls of semilinear parabolic equation where some data of the heat equation are incomplete and unknown (see also [6] for the heat equation in presence of superlinear nonlinearity) and [34] when the control and the observation regions are disjoint. When focusing on hyperbolic systems and fluid mechanics, similar works have been carried out, see in particular [2, 10] for the wave equation, [17] for a simplified linear ocean model, [21, 22] for recent papers on Stokes and Navier–Stokes equations.

Previous papers on this topic address a local sensitivity problem, that is they study the derivative of the quantity of interest around a given value of one parameter. The work we propose here presents a double originality. Firstly we will address simultaneously the sensitivity to all uncertain parameters, and not just one. And secondly, we propose to investigate the global sensitivity, when the parameters vary around their mean values, following prescribed probability distributions (Gaussian or uniform). Therefore, the present approach can be seen as a global analysis of the control. This will be addressed using statistical techniques.

Sensitivity analysis aims to find the most sensitive parameters, i.e. parameters whose variations have the largest impact on the output quantity. Local sensitivity analysis essentially computes the derivative of the output with respect to the parameter, at a given value of the parameter. Global (stochastic) sensitivity analysis (see e.g. [39] for a review) assumes that the parameters can vary widely, either in a given range, or around a given value. In this framework, the parameters are assumed to follow suitable probability distributions. One way of measuring sensitivities is to compute sensitivity indices, such as Sobol indices [43], which quantify the contribution of a given parameter or set of parameters to the output variance: the larger the index value, the greater the sensitivity.

These indices are in general impossible to compute exactly, and must be estimated. Classical approaches of effective computation use Monte-Carlo type methods, see the survey [24]. We can cite the FAST method (Fourier Amplitude Sensitivity Testing, [9, 46]) which uses the Fourier decomposition of the output function, the polynomial chaos expansion method [45], and the Sobol pick-freeze scheme [43, 44, 28, 18] which uses sampled replications of model outputs. The Monte-Carlo approach requires a large number of model runs (e.g. around one thousand for one parameter). As in general the model is complex and requires large computing time, it is beneficial to replace the full model by a metamodel, that is an approximate but fast model. In this work we used the reduced basis method [19, 20, 36, 47, 29], but we can also mention kriging

method [40], interpolation kernels [41], and we refer to [16] for a review on metamodeling methods. The reduced basis method consists in solving the discrete model partial differential equation in a smaller dimension space, i.e. to look for a solution in a space spanned by a reduced basis instead of a large generic basis (such as finite elements). The advantage of this method is that it can provide certified error bounds that allow us to quantify the information loss between the full model and the metamodel, and therefore to provide certified Confidence Intervals (CI) for the sensitivity indices [30].

This paper is organized as follows. Section 2 presents the model and states the problem. Section 3 presents the sensitivity analysis in our context, and describes the numerical computation of indices using Monte Carlo approach and reduced basis metamodeling. Section 4 presents numerical results. We conclude and give outlooks in Section 5. The Appendix collects the proof of some intermediate results. This work is an extension of the paper of the same title presented at the 2014 CDC conference [32], where no proof is given, a simpler to-be-controlled output is considered and less parameters are included in the sensitivity analysis.

2 Boundary control of an open channel and problem statement

2.1 Quasilinear equation

Let us consider the classical Shallow Water equations describing the flow dynamics inside of an open-channel. For an introduction of such model and related control problems see e.g. [7, 3, 14]. This model describes the space and time-evolution of the water depth $H = H(x, t)$ and horizontal water velocity $V = V(x, t)$, for all $(x, t) \in [0, L] \times \mathbb{R}_+$, and is written as follows

$$\partial_t \begin{pmatrix} H \\ V \end{pmatrix} + \partial_x \begin{pmatrix} HV \\ \frac{1}{2}V^2 + gH \end{pmatrix} + \begin{pmatrix} 0 \\ g(S_f - S_b) \end{pmatrix} = 0, \quad (1)$$

where L stands for the length of the pool, g is the gravity constant, S_b is the bottom slope and S_f is the friction slope. Moreover it is assumed that the bottom slope S_b doesnot depend on x .

Let us denote the water flow by Q . It is given by $Q(x, t) = BH(x, t)V(x, t)$ where B is a constant channel width. In the present work, we suppose there are two gates, one at $x = 0$ and one at $x = L$, which are respectively

- a submerged underflow gate:

$$Q(0, t) = U_0 B \mu_0 \sqrt{2g(z_{up} - H(0, t))}, \quad (2)$$

where z_{up} is the water level before the gate, μ_0 the water flow coefficient and U_0 the position of the spillway (see Figure 1),

– a submerged overflow gate:

$$H(L, t) = \left(\frac{Q^2(L, t)}{2gB^2\mu_L^2} \right)^{1/3} + h_s + U_L, \quad (3)$$

where h_s is the height of the fixed part of the overflow gate, μ_L the water flow coefficient at this gate and U_L the position of the spillway (see Figure 1).

The controls are the positions U_0 and U_L of both spillways located at the extremities of the pool and related to the state variables H and Q .

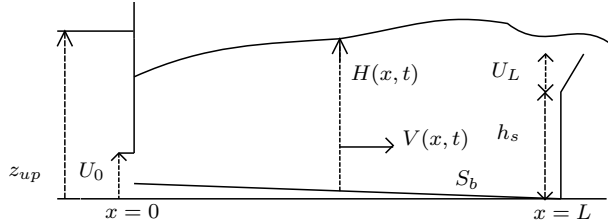


Fig. 1 Sketch of a channel: one reach with a downstream overflow gate and an upstream underflow gate.

Other kinds of boundary conditions (BC) can be considered e.g., two submerged underflow gates (or two submerged overflow gates) at $x = 0$ and at $x = L$.

There are sufficient stability conditions written in terms of the boundary conditions for the stability of (1) with the boundary conditions (2)-(3). These sufficient conditions exploit Lyapunov functions (see e.g. [8]), or analysis of the characteristic curves (see [37,33]).

There are various empirical models that are available in the literature for the friction slope (see e.g. [4,14] which are considering two different models). Let us pick the model of [4] for S_f , that is

$$S_f = C \frac{V^2}{H}, \quad (4)$$

where C is a constant friction coefficient.

2.2 Linearized model and stabilizing control laws

A steady-state solution or *equilibrium* of (1) is a time-independent solution of this equation. Let us consider a space-independent equilibrium, denoted H^*, V^* and defined by:

$$V^* = \left(\frac{S_b Q^*}{BC} \right)^{1/3}, \quad H^* = \frac{Q^*}{BV^*}. \quad (5)$$

Using (1) and (4), it implies $S_f = S_b$ and $S_b H^* = C(V^*)^2$. The linearized Shallow Water equations around such an equilibrium are computed in [4]. Denoting the deviations of the state with respect to such an equilibrium by $h(x, t) = H(x, t) - H^*$ and $v(x, t) = V(x, t) - V^*$, we have:

$$\partial_t \begin{pmatrix} h \\ v \end{pmatrix} + \begin{pmatrix} V^* & H^* \\ g & V^* \end{pmatrix} \partial_x \begin{pmatrix} h \\ v \end{pmatrix} + \begin{pmatrix} 0 & 0 \\ -\frac{gS_b}{H^*} & \frac{2gS_b}{V^*} \end{pmatrix} \begin{pmatrix} h \\ v \end{pmatrix} = 0 ,$$

or equivalently, by recalling that $S_b H^* = C(V^*)^2$,

$$\partial_t \begin{pmatrix} h \\ v \end{pmatrix} + \begin{pmatrix} V^* & H^* \\ g & V^* \end{pmatrix} \partial_x \begin{pmatrix} h \\ v \end{pmatrix} + \begin{pmatrix} 0 & 0 \\ -\frac{gC(V^*)^2}{(H^*)^2} & \frac{2gCV^*}{H^*} \end{pmatrix} \begin{pmatrix} h \\ v \end{pmatrix} = 0 . \quad (6)$$

We now introduce the classical characteristic coordinates defined by:

$$\begin{aligned} \xi_1(x, t) &= v(x, t) + h(x, t) \sqrt{\frac{g}{H^*}} \\ \xi_2(x, t) &= v(x, t) - h(x, t) \sqrt{\frac{g}{H^*}} \end{aligned} \quad (7)$$

for all $(x, t) \in [0, L] \times \mathbb{R}_+$, and the characteristic velocities:

$$\lambda_1 = V^* + \sqrt{gH^*} , \quad -\lambda_2 = V^* - \sqrt{gH^*} . \quad (8)$$

Assume that the flow is fluvial, that is $gH^* > V^{*2}$. Under this condition, the characteristic velocities have opposite signs, that is $\lambda_1 > 0$ and $-\lambda_2 < 0$.

The linearized Shallow Water equations (6) may be rewritten as

$$\partial_t \begin{pmatrix} \xi_1 \\ \xi_2 \end{pmatrix} + \begin{pmatrix} \lambda_1 & 0 \\ 0 & -\lambda_2 \end{pmatrix} \partial_x \begin{pmatrix} \xi_1 \\ \xi_2 \end{pmatrix} + \begin{pmatrix} \gamma & \delta \\ \gamma & \delta \end{pmatrix} \begin{pmatrix} \xi_1 \\ \xi_2 \end{pmatrix} = 0 \quad (9)$$

with the parameters

$$\begin{aligned} \gamma &= gC \frac{(V^*)^2}{H^*} \left(\frac{1}{V^*} - \frac{1}{2\sqrt{gH^*}} \right) , \\ \delta &= gC \frac{(V^*)^2}{H^*} \left(\frac{1}{V^*} + \frac{1}{2\sqrt{gH^*}} \right) . \end{aligned} \quad (10)$$

We then have the following proposition (see Appendix A.1 for the proof which is inspired by [14,4]):

Proposition 1 *Given any constant values k_0 and k_L , let us define the controls U_0 and U_L by, for all $t \geq 0$,*

$$U_0(t) = \frac{H(0, t) \left(V^* - \frac{1+k_0}{1-k_0} (H(0, t) - H^*) \sqrt{\frac{g}{H^*}} \right)}{\mu_0 \sqrt{2g(z_{up} - H(0, t))}} ; \quad (11)$$

$$U_L(t) = - \left(\frac{H(L, t) \left(V^* + \frac{1+k_L}{1-k_L} (H(L, t) - H^*) \sqrt{\frac{g}{H^*}} \right)}{\sqrt{2g}\mu_L} \right)^{\frac{2}{3}} + H(L, t) - h_s . \quad (12)$$

Then the boundary conditions (2) and (3) may be rewritten as

$$\begin{pmatrix} \xi_1(0, t) \\ \xi_2(L, t) \end{pmatrix} = \begin{pmatrix} 0 & k_0 \\ k_L & 0 \end{pmatrix} \begin{pmatrix} \xi_1(L, t) \\ \xi_2(0, t) \end{pmatrix}. \quad (13)$$

Note that by defining the to-be-measured outputs as the water heights at both extremities of the channel, namely $H(0, t)$, and $H(L, t)$, the previous result defines output feedback controllers U_0 and U_L . Moreover, note that this is an exact expression (not coming from an approximation or a linearization of the boundary conditions (2) and (3)).

It is possible to combine the previous results with Lyapunov techniques to compute stabilizing controllers. This is one of the contributions of [4] which is recalled here:

Proposition 2 ([4]) *For any $(k_0, k_L) \in \mathbb{R}$ such that*

$$\max \left\{ |k_0| \sqrt{\frac{\lambda_1 \gamma}{\lambda_2 \delta}}, |k_L| \sqrt{\frac{\lambda_2 \delta}{\lambda_1 \gamma}} \right\} < 1, \quad (14)$$

where γ and δ are defined in (10), defining U_0 and U_L with Proposition 1, the system (9) with the boundary conditions (13) is exponentially stable (in L^2 -norm). More precisely, there exist $\nu > 0$ and $M > 0$ such that, for every initial condition $(\xi_1^0, \xi_2^0) \in L^2((0, L); \mathbb{R}^2)$, the solution to the Cauchy problem (9) with the boundary conditions (13) and the initial condition

$$(\xi_1(x, 0), \xi_2(x, 0)) = (\xi_1^0(x), \xi_2^0(x)), \quad \forall x \in (0, L) \quad (15)$$

satisfies

$$\|(\xi_1(\cdot, t), \xi_2(\cdot, t))\|_{L^2((0, L); \mathbb{R}^2)} \leq M e^{-\nu t} \|(\xi_1^0, \xi_2^0)\|_{L^2((0, L); \mathbb{R}^2)}.$$

The proof of the previous result is given in [4] by noting that (14) is equivalent to [4, Condition (9)].

2.3 Problem statement

Assume now that we want to use this study to compute a stabilizing control for a real-life channel. In this case, a legitimate question to ask is whether the controls computed using the theoretical model and Propositions 1 and 2 are accurate enough to stabilize the real-life channel. More specifically, most of the physical parameters in this problem are measured quantities, potentially endowed with measurement errors. Thus the theoretical channel may differ from the real-life one. And as the control has been designed on the theoretical channel, it may lead to a difference in the quality of the stabilization of the real-life (or uncertain) channel. In this paper, we want to find which physical parameters have the largest influence on this quality of stabilization.

Indeed, if there are measurement errors, the real-life model is still governed by (9), but the true values for the parameters are unknown, *a priori* different

from the nominal values used to model the theoretical channel. Moreover some parameters in (1) are not well modeled, e.g., the friction slope S_f , given by (4), for which others models exist in the literature (see e.g. [4] and [14]). The only way to design the control is to use for each parameter its nominal value. It leads to nonlinear boundary conditions, which we linearize in order to keep the resolution simple. Let us denote with *nom* in subscript the nominal value of a parameter. For instance, $z_{up,nom}$ is the nominal value of z_{up} . The quantities V_{nom}^* and H_{nom}^* are defined by (5), with all parameters fixed to their nominal values. We obtain the following proposition (see Appendix A.2 for the proof):

Proposition 3 *Given any constant values k_0 and k_L , let us define the controls U_0 and U_L by, for all $t \geq 0$,*

$$U_0(t) = \frac{H(0,t) \left(V_{nom}^* - \frac{1+k_0}{1-k_0} (H(0,t) - H_{nom}^*) \sqrt{\frac{g}{H_{nom}^*}} \right)}{\mu_0 \sqrt{2g} (z_{up,nom} - H(0,t))} \quad (16)$$

$$U_L(t) = - \left(\frac{H(L,t) \left(V_{nom}^* + \frac{1+k_L}{1-k_L} (H(L,t) - H_{nom}^*) \sqrt{\frac{g}{H_{nom}^*}} \right)}{\sqrt{2g} \mu_L} \right)^{\frac{2}{3}} + H(L,t) - h_{s,nom}. \quad (17)$$

Then the boundary conditions (2) and (3) for the real-life model (9) are linearized as:

$$\left(1 - \frac{\mathcal{B} + \sqrt{g/H^*}}{2\sqrt{g/H^*}} \right) \xi_1(0,t) + \frac{\mathcal{B} + \sqrt{g/H^*}}{2\sqrt{g/H^*}} \xi_2(0,t) = \mathcal{A} \quad (18)$$

$$-\frac{\mathcal{D} - \sqrt{g/H^*}}{2\sqrt{g/H^*}} \xi_1(L,t) + \left(1 + \frac{\mathcal{D} - \sqrt{g/H^*}}{2\sqrt{g/H^*}} \right) \xi_2(L,t) = \mathcal{C} \quad (19)$$

where \mathcal{A} , \mathcal{B} , \mathcal{C} and \mathcal{D} are values defined in Appendix A.2.

Remark 1 We remark that if the nominal parameters coincide with the true ones, Proposition 1 and Proposition 3 provide the same boundary conditions.

Let us define by $\mu = (h_s, B, S_b, C, z_{up}, \xi_1^0, \xi_2^0, \mu_0, \mu_L)$ the vector of uncertain parameters. We consider in the following that the uncertainties on these parameters can be considered independent of each other. We then assume that the errors in measurement for parameters h_s , B , S_b , z_{up} , μ_0 and μ_L are governed by independent Gaussian random variables. For each of these Gaussian variables, the expectation is the nominal value of the parameter and the standard deviation reflects the precision of the measurements. A small standard deviation is chosen if we consider that measurements are precise. Initial conditions (ξ_1^0, ξ_2^0) and parameter C (defining the friction slope in (4)) are modeled by uniform distributions. It is a common choice when only bounds on the uncertainty distribution is assumed. However, it is important to note here that

the whole methodology we develop in this paper can be generalized to any choice of probability distributions for the parameters, as soon as the uncertainties on the various parameters can be assumed independent of each other. For measurements errors, we could also have considered truncated Gaussian distributions to ensure the positivity of the parameters. In many fields of application (e.g., meteorological, oceanography, ...), it happens that the data are observed indirectly through some nonlinear observation mapping, and after some preprocessing. In that case, uncertainty modeling may involve non trivial probability distributions. In Section 4, we arbitrarily choose numerical values for the expectations and variances of the probability distributions modeling the uncertainty of parameters h_s , B , S_b , C , z_{up} , ξ_1^0 , ξ_2^0 , μ_0 and μ_L (see Table 1).

The stability of the system is then evaluated by the so-called *to-be-controlled output*:

$$f(\mu) = \sqrt{\int_{t=0}^{T^*} \int_{x=0}^L \xi_1(x,t)^2 + \xi_2(x,t)^2 dx dt}, \quad (20)$$

where T^* is a given time horizon. In our study, the parameters (k_0, k_L) will be fixed by the controller. Recall that ξ is governed by Equation (9) with boundary conditions given by Proposition 3. The sensitivity of the *to-be-controlled output* to the input parameters μ will be derived by performing a global sensitivity analysis whose bases are recalled in the next section. The closed-loop system is sketched out in Figure 2, and in Figure 3 where the uncertainties appear.

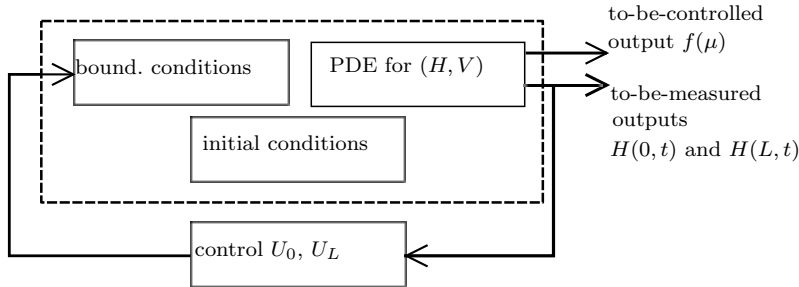


Fig. 2 Control loop in case when are no uncertainties.

3 Sensitivity analysis

In the following, one wants to measure the sensitivity of the *to-be-controlled output* $f(\mu)$ with respect to the uncertainties on the parameter vector μ .

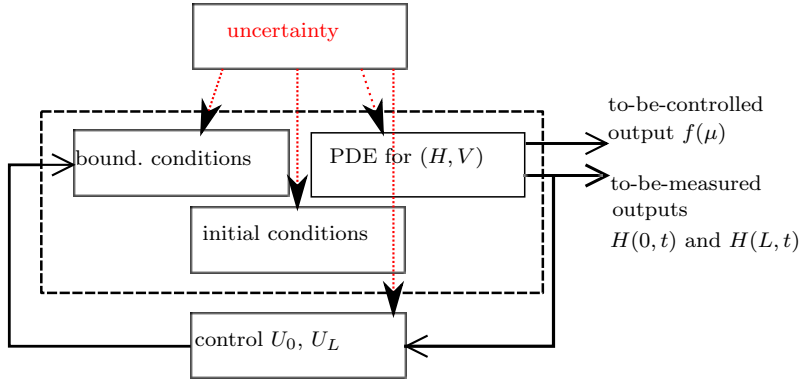


Fig. 3 Control loop in case of uncertainties.

3.1 Global sensitivity: a variance-based approach

We adopt a stochastic framework. Input parameters μ_1, \dots, μ_p (here $p = 9$) are assumed to be independent and are thus modeled by one-dimensional distributions, as detailed in Section 2.3. The *to-be-controlled output* can then be considered as a scalar random variable $Y = f(\mu)$. We assume that Y is square integrable and non deterministic in the sense that $\text{Var}(Y) \neq 0$.

The conditional expectation $\mathbb{E}(Y|\mu_i)$ is a random variable which gives the mean of Y over the distributions of the μ_j ($j \neq i$), when μ_i is fixed. It is the best approximation in the mean square sense of Y which depends on μ_i only. Its variance quantifies the influence of μ_i on the dispersion of Y . The Sobol' sensitivity indices are obtained by normalizing this variance, by the total variance of the *to-be-controlled output*, Y . Thus, the Sobol' first order sensitivity index of input parameter μ_i is defined by

$$S_{\{i\}} = \frac{\text{Var}(\mathbb{E}(Y|\mu_i))}{\text{Var}(Y)}.$$

It belongs to the interval $[0, 1]$.

More generally, one can define sensitivity indices of any order $r \in \{1, \dots, p\}$, starting from the functional Analysis Of Variance (ANOVA) decomposition (see [25] and [15]). Let us first introduce some notations. We assume that f is a real square integrable function, \mathbf{u} is a subset of $\{1, \dots, p\}$, \mathbf{u}^c stands for its complement, its cardinal is denoted $r = |\mathbf{u}|$, and $\mu_{\mathbf{u}}$ represents the random vector with components μ_i , $i \in \mathbf{u}$. The ANOVA decomposition then states that $Y = f(\mu)$ can be uniquely decomposed into summands of increasing dimensions

$$f(\mu) = \sum_{\mathbf{u} \subseteq \{1, \dots, p\}} f_{\mathbf{u}}(\mu_{\mathbf{u}}) \quad (21)$$

where $f_\emptyset = \mathbb{E}[Y]$ and the other components have zero mean value and are mutually uncorrelated. From (21) and its properties, we deduce that

$$\begin{aligned} \mathbb{E}(f(\mu) - f_\emptyset)^2 &= \text{Var}(Y) \\ &= \sum_{\mathbf{u} \subseteq \{1, \dots, p\}, \mathbf{u} \neq \emptyset} \text{Var}(f_{\mathbf{u}}(\mu_{\mathbf{u}})) . \end{aligned}$$

For any $\mathbf{v} \subseteq \{1, \dots, p\}$, let $|\mathbf{v}|$ denote the cardinal of \mathbf{v} . The Sobol' index [43] of order $r = |\mathbf{u}|$ with respect to the combination of all the variables in $\mathbf{u} \subseteq \{1, \dots, p\}$ is then defined as

$$S_{\mathbf{u}} = \frac{\sigma_{\mathbf{u}}^2}{\sigma^2} = \frac{\text{Var}[f_{\mathbf{u}}(\mu_{\mathbf{u}})]}{\text{Var}[Y]} . \quad (22)$$

The main effect of the i^{th} factor is measured by $S_{\{i\}}$. Then, for $i \neq j$, the interaction effect due to the i^{th} and the j^{th} factors, that cannot be explained by the sum of the individual effects of μ_i and μ_j , is measured by $S_{\{i,j\}}$, and so on (see [39]). Note that the Sobol' index of order $r = |\mathbf{u}|$ with respect to the combination of all the variables in $\mathbf{u} \subseteq \{1, \dots, p\}$ can also be written in the following more intuitive form

$$S_{\mathbf{u}} = \frac{\sum_{\mathbf{v} \subseteq \mathbf{u}} (-1)^{|\mathbf{u}|-|\mathbf{v}|} \text{Var}[\mathbb{E}(Y | \mu_i, i \in \mathbf{v})]}{\text{Var}[Y]} .$$

It is straightforward to prove that, $\forall \mathbf{u} \subseteq \{1, \dots, p\}$,

$$0 \leq S_{\mathbf{u}} \leq 1, \quad \sum_{\mathbf{u} \subseteq \{1, \dots, p\}} S_{\mathbf{u}} = 1 .$$

For any $i \in \{1, \dots, p\}$, we also define a total sensitivity index $S_{\{i\}}^{\text{tot}}$ [26] to express the overall output sensitivity to an input μ_i by

$$S_{\{i\}}^{\text{tot}} = \sum_{\mathbf{v} \subseteq \{1, \dots, p\} \text{ such that } i \in \mathbf{v}} S_{\mathbf{v}} . \quad (23)$$

From (23) we deduce that

$$0 \leq S_{\{i\}} \leq S_{\{i\}}^{\text{tot}} \leq 1 .$$

If $S_{\{i\}} = S_{\{i\}}^{\text{tot}}$, then it means that the input μ_i has no interaction with other inputs.

For practical purposes, we also define the closed Sobol' index of order $r = |\mathbf{u}|$ with respect to the combination of all the variables in $\mathbf{u} \subseteq \{1, \dots, p\}$ as

$$S_{\mathbf{u}}^{\text{closed}} = \sum_{\mathbf{v} \subseteq \mathbf{u}} S_{\mathbf{v}} . \quad (24)$$

We have

$$0 \leq S_{\mathbf{u}}^{\text{closed}} = \frac{\text{Var}[\mathbb{E}(Y | \mu_i, i \in \mathbf{u})]}{\text{Var}[Y]} \leq 1 .$$

Let us remark that for first-order indices, $S_{\{i\}}^{\text{closed}}$ and $S_{\{i\}}$ coincide. For $i \neq j$, the interaction effect due to the i^{th} and the j^{th} factors, including the part which can be explained by the sum of the individual effects of μ_i and μ_j , is thus measured by $S_{\{i,j\}}^{\text{closed}}$.

In our context, as in many contexts, no analytical formula is available for the Sobol' indices, which we thus need to estimate.

3.2 An estimator for Sobol' indices

In this subsection, we introduce the classical Monte Carlo estimator of Sobol' indices first introduced in [43].

We first need some notation. Let \mathbb{P}_μ be the probability distribution of the random vector μ . Let \mathbf{u} be a non-empty subset of $\{1, \dots, p\}$. For any $i \in \{1, \dots, p\}$, let μ'_i be a random variable distributed as μ_i and independent of μ_i . Recall that the p parameters μ_1, \dots, μ_p are independently distributed according to Section 2.3. Define $\mu_{\mathbf{u}} = (\mu_i, i \in \mathbf{u})$, $\mu'_{\mathbf{u}^c} = (\mu'_i, i \in \mathbf{u}^c)$. Consider $Y_{\mathbf{u}} = f(\mu_{\mathbf{u}}, \mu'_{\mathbf{u}^c})$. From Lemma 1.2 in [28] we know that

$$S_{\mathbf{u}}^{\text{closed}} = \frac{\text{Cov}(Y, Y_{\mathbf{u}})}{\text{Var}[Y]}. \quad (25)$$

Then, to define an estimator of $S_{\mathbf{u}}^{\text{closed}}$, it seems intuitive to replace in (25) the term $\text{Cov}(Y, Y_{\mathbf{u}})$ (*resp.* $\text{Var}[Y]$) by some empirical version.

For that purpose, let us introduce, for any $i \in \{1, \dots, p\}$, $\mu_i^{j,1}$ and $\mu_i^{j,2}$, $j = 1, \dots, n$ two *independent and identically distributed* (i.i.d.) samples of size n of the parameter μ_i . We now define

$$\begin{aligned} \mu_{\mathbf{u}}^j &= (\mu_i^{j,1}, i \in \mathbf{u}) \\ \mu_{\mathbf{u}^c}^{j,1} &= (\mu_i^{j,1}, i \in \mathbf{u}^c) \\ \mu_{\mathbf{u}^c}^{j,2} &= (\mu_i^{j,2}, i \in \mathbf{u}^c). \end{aligned}$$

Finally, for $k = 1$ and 2 , consider

$$Y_{\mathbf{u}}^{j,k} = f(\mu_{\mathbf{u}}^j, \mu_{\mathbf{u}^c}^{j,k}).$$

We define the estimator $\hat{S}_{\mathbf{u},n}^{\text{closed}}$ of $S_{\mathbf{u}}^{\text{closed}}$ as

$$\hat{S}_{\mathbf{u},n}^{\text{closed}} = \frac{\frac{1}{n} \sum_{j=1}^n Y_{\mathbf{u}}^{j,1} Y_{\mathbf{u}}^{j,2} - \left(\frac{1}{n} \sum_{j=1}^n \frac{Y_{\mathbf{u}}^{j,1} + Y_{\mathbf{u}}^{j,2}}{2} \right)^2}{\frac{1}{n} \sum_{j=1}^n \frac{(Y_{\mathbf{u}}^{j,1})^2 + (Y_{\mathbf{u}}^{j,2})^2}{2} - \left(\frac{1}{n} \sum_{j=1}^n \frac{Y_{\mathbf{u}}^{j,1} + Y_{\mathbf{u}}^{j,2}}{2} \right)^2} \quad (26)$$

with $\mathbf{u} = \{i\}$ for first-order indices and $\mathbf{u} = \{i, j\}$ for closed second-order indices. This estimator was first introduced in [35]. Various choices were possible

for the empirical version of $\text{Cov}(Y, Y_{\mathbf{u}})$ (*resp.* $\text{Var}[Y]$). The choice considered in (26) above ensures good asymptotic properties for the estimator $\hat{S}_{\mathbf{u},n}^{\text{closed}}$ of $S_{\mathbf{u}}^{\text{closed}}$. These asymptotic properties are stated in [28, Propositions 2.2 and 2.5].

This estimator requires a large number n of model evaluations. Therefore, to reduce the cost, we opt for a metamodel approach, replacing Equation (9) by a reduction of (9). We refer to Section 3.3 for more details on the reduction procedure. Let us now define the respective estimators of $S_{\{i\}}$ and $S_{\{i\}}^{\text{tot}}$ as

$$\hat{S}_{\{i\},n} = \hat{S}_{\{i\},n}^{\text{closed}}, \hat{S}_{\{i\},n}^{\text{tot}} = 1 - \hat{S}_{\{i\}^c,n}^{\text{closed}}.$$

Thanks to [28] we can state the following theorem, which gives asymptotic confidence intervals for the Sobol' indices:

Theorem 1 *Assume that $\mathbb{E}(Y^4) < \infty$. Let $\alpha \in (0, 1)$ (typically $\alpha = 0.05$ or 0.10). Let $\mathbf{u} \subseteq \{1, \dots, p\}$ and $i \in \{1, \dots, p\}$.*

(i) *Let $v_{\mathbf{u}}$ be defined by*

$$v_{\mathbf{u}}^2 = \frac{\text{Var}((Y - \mathbb{E}Y)(Y_{\mathbf{u}} - \mathbb{E}Y) - \frac{S_{\mathbf{u}}}{2}((Y - \mathbb{E}Y)^2 + (Y_{\mathbf{u}} - \mathbb{E}Y)^2))}{(\text{Var}Y)^2}. \quad (27)$$

Then, for any consistent estimator $\hat{v}_{\mathbf{u}}$ of $v_{\mathbf{u}}$, an asymptotic confidence interval (CI) of level $1 - \alpha$ for $S_{\mathbf{u}}^{\text{closed}}$ is given by

$$\left[\hat{S}_{\mathbf{u},n}^{\text{closed}} - z_{1-\frac{\alpha}{2}} \frac{\hat{v}_{\mathbf{u}}}{\sqrt{n}}, \hat{S}_{\mathbf{u},n}^{\text{closed}} + z_{1-\frac{\alpha}{2}} \frac{\hat{v}_{\mathbf{u}}}{\sqrt{n}} \right],$$

with $z_{1-\frac{\alpha}{2}}$ is the $1 - \frac{\alpha}{2}$ quantile of the $\mathcal{N}(0, 1)$;

(ii) *Let $v_{\sim i}^2$ be defined by (27) with $\mathbf{u} = \{1, \dots, i-1, i+1, \dots, p\}$. Then, for any consistent estimator $\hat{v}_{\sim i}$ of $v_{\sim i}$, an asymptotic CI of level $1 - \alpha$ for $S_{\{i\}}^{\text{tot}}$ is given by*

$$\left[\hat{S}_{\{i\},n}^{\text{tot}} - z_{1-\frac{\alpha}{2}} \frac{\hat{v}_{\sim i}}{\sqrt{n}}, \hat{S}_{\{i\},n}^{\text{tot}} + z_{1-\frac{\alpha}{2}} \frac{\hat{v}_{\sim i}}{\sqrt{n}} \right],$$

with $z_{1-\frac{\alpha}{2}}$ is the $1 - \frac{\alpha}{2}$ quantile of the $\mathcal{N}(0, 1)$ distribution.

Proof of Theorem 1. From [28, Proposition 2.2], we get that

$$\sqrt{n} \left(\hat{S}_{\mathbf{u},n}^{\text{closed}} - S_{\mathbf{u}}^{\text{closed}} \right) \xrightarrow[n \rightarrow +\infty]{\mathcal{D}} \mathcal{N}(0, v_{\mathbf{u}}^2)$$

with $v_{\mathbf{u}}^2$ defined by (27). Then, using Slutsky's Lemma, we get the result in Item (i) of Theorem 1 for $S_{\mathbf{u}}$. Moreover, note that $S_{\{i\}}^{\text{tot}} = 1 - S_{\sim i}^{\text{closed}}$ with $\sim i = \{1, \dots, i-1, i+1, \dots, p\}$. We thus get the result in Item (ii) for $S_{\{i\}}^{\text{tot}}$. \square

Assume now that we approximate the true model f by a metamodel \tilde{f} . In the following we will consider reduced basis metamodeling (see Section 3.3 below). For $k = 1$ and 2 , we now consider

$$\tilde{Y}_{\mathbf{u}}^{j,k} = \tilde{f}(\mu_{\mathbf{u}}^j, \mu_{\mathbf{u}^c}^{j,k}). \quad (28)$$

We define $\tilde{S}_{u,n}^{\text{closed}}$ as in (26) by replacing Y by \tilde{Y} . Using the results in [28] we have the following confidence intervals for the Sobol indices, using now the estimator based on the metamodel:

Corollary 1 *Assume that the metamodel \tilde{f} depends on the Monte-Carlo sample size n , that there exists $c \in \mathbb{R}$ such that $\tilde{f}_n(\mu) - f(\mu) \xrightarrow[n \rightarrow +\infty]{\mathbb{L}^2(\mathbb{P}_\mu)} c$, and that $n \text{Var} \left(\tilde{f}_n(\mu) - f(\mu) \right) \xrightarrow[n \rightarrow +\infty]{} 0$. Assume that $\mathbb{E}(Y^4) < \infty$. Let $\alpha \in (0, 1)$ (typically $\alpha = 0.05$ or 0.10). Let $\mathbf{u} \subseteq \{1, \dots, p\}$ and $i \in \{1, \dots, p\}$. Then,*

(i) *for any consistent estimator \hat{v}_u of v_u , where v_u^2 is defined by (27), an asymptotic CI of level $1 - \alpha$ for S_u^{closed} is given by*

$$\left[\tilde{S}_{u,n}^{\text{closed}} - z_{1-\frac{\alpha}{2}} \frac{\hat{v}_u}{\sqrt{n}}, \tilde{S}_{u,n}^{\text{closed}} + z_{1-\frac{\alpha}{2}} \frac{\hat{v}_u}{\sqrt{n}} \right],$$

with $z_{1-\frac{\alpha}{2}}$ is the $1 - \frac{\alpha}{2}$ quantile of the $\mathcal{N}(0, 1)$ distribution;

(ii) *for any consistent estimator $\hat{v}_{\sim i}$ of $v_{\sim i}$, where $v_{\sim i}^2$ is defined by (27) with $\sim i = \{1, \dots, i-1, i+1, \dots, p\}$, an asymptotic CI of level $1 - \alpha$ for $S_{\{i\}}^{\text{tot}}$ is given by*

$$\left[\tilde{S}_{\{i\},n}^{\text{tot}} - z_{1-\frac{\alpha}{2}} \frac{\hat{v}_{\sim i}}{\sqrt{n}}, \tilde{S}_{\{i\},n}^{\text{tot}} + z_{1-\frac{\alpha}{2}} \frac{\hat{v}_{\sim i}}{\sqrt{n}} \right],$$

with $z_{1-\frac{\alpha}{2}}$ is the $1 - \frac{\alpha}{2}$ quantile of the $\mathcal{N}(0, 1)$ distribution.

Proof of Corollary 1. Let $\mathbf{u} \subseteq \{1, \dots, p\}$. From Item (1) of Theorem 3.4 in [28], we know that

$$\sqrt{n} \left(\tilde{S}_{u,n}^{\text{closed}} - S_u^{\text{closed}} \right) \xrightarrow[n \rightarrow +\infty]{\mathcal{D}} \mathcal{N} \left(0, v_u^2 \right)$$

as $n \|\tilde{f}_n - f\|_\infty \xrightarrow[n \rightarrow +\infty]{} 0$, where v_u^2 is the limit variance in Theorem 1. Then applying Slutsky's Lemma, it yields the result in Item (i).

Item (ii) for $S_{\{i\}}^{\text{tot}}$ is obtained by noting that $S_{\{i\}}^{\text{tot}} = 1 - S_{\sim i}^{\text{closed}}$. \square

3.3 Discretized and reduced model

3.3.1 Discretization of the model

We use an implicit upwind scheme to discretize (9). We denote by $k = 1, \dots, N_t$ the discrete time index, by $i = 1, \dots, N_x$ the space index (where N_x and N_t are the numbers of discretization points in space and time respectively), and by $\xi_j^{i,k}$ an approximation of ξ_j ($j = 1, 2$) at the i th point of the uniform space grid on $[0, L]$ with N_x points and at the k th timestep. We denote by $\Delta x = L/N_x$ and $\Delta t = T^*/N_t$ the space and time steps, respectively.

Using a classical upwind scheme, we get the following approximations:

$$\partial_t \xi_1 + \lambda_1 \partial_x \xi_1 \approx \left(\frac{\xi_1^{i,k+1} - \xi_1^{i,k}}{\Delta t} + \lambda_1 \frac{\xi_1^{i,k+1} - \xi_1^{i-1,k+1}}{\Delta x} \right)_{i,k}$$

and:

$$\partial_t \xi_2 - \lambda_2 \partial_x \xi_2 \approx \left(\frac{\xi_2^{i,k+1} - \xi_2^{i,k}}{\Delta t} - \lambda_2 \frac{\xi_2^{i+1,k+1} - \xi_2^{i,k+1}}{\Delta x} \right)_{i,k},$$

which give, when combined to (9), the following implicit recurrence (in k) relations:

$$\begin{aligned} \left(\frac{1}{\Delta t} + \frac{\lambda_1}{\Delta x} + \gamma \right) \xi_1^{i,k+1} - \frac{\lambda_1}{\Delta x} \xi_1^{i-1,k+1} + \delta \xi_2^{i,k+1} &= \frac{\xi_1^{i,k}}{\Delta t} \\ \left(\frac{1}{\Delta t} - \frac{\lambda_2}{\Delta x} + \delta \right) \xi_2^{i,k+1} + \frac{\lambda_2}{\Delta x} \xi_2^{i,k+1} + \gamma \xi_1^{i,k+1} &= \frac{\xi_2^{i,k}}{\Delta t}. \end{aligned}$$

The boundary conditions (18) and (19) can readily be incorporated so as to write, at each time step, a linear system of equations that has to be solved so as to find ξ_1^{k+1} and ξ_2^{k+1} from ξ_1^k and ξ_2^k .

3.3.2 Discrete output

An approximation of the *to-be-controlled output* can then be obtained by discretizing the double integral in (20):

$$f_{\text{discrete}}(\mu) = \sqrt{\sum_{i=1}^{N_x} \sum_{k=0}^{N_t} \left(\xi_1^{i,k} \right)^2 + \left(\xi_2^{i,k} \right)^2}$$

Notice that we do not include the $1/(N_x \times (N_t + 1))$ normalization factor, as this will not change the Sobol indices.

3.3.3 Model reduction and error bound

As the experimental model will have to be numerically solved for a large number of parameter values, we use the *reduced basis* technique (see e.g., [36], and [31] for space-time reduction) so as to accelerate the resolutions of the above mentioned systems. We use a space-time reduced basis approach, which can be summed up as follows: we introduce the vector $\xi = (\xi_1^0, \xi_2^0, \xi_1^1, \xi_2^1, \dots, \xi_1^{N_t}, \xi_2^{N_t})$ in $\mathbb{R}^{\mathcal{N}}$ (with $\mathcal{N} = 2 \times (N_t + 1) \times N_x$), which is the solution of the large dimensional problem $A(\mu)\xi = b(\mu)$, where $A(\mu)$ and $b(\mu)$ are appropriate functions of the true parameter values μ . One can check that $A(\mu)$ and $b(\mu)$ satisfy the so-called affine decomposition hypothesis (as described in [36]), hence the classical reduced basis algorithms (op. cit.) can be readily applied to this system, leading to a reduced solution $\tilde{\xi}$ of the linear system:

$$\tilde{A}(\mu)\tilde{\xi} = \tilde{b}(\mu),$$

where $\tilde{A}(\mu)$ is a square matrix of dimension $m \ll \mathcal{N}$, and $\tilde{\xi}, \tilde{b}(\mu) \in \mathbb{R}^m$. An approximation of $\xi(\mu)$ can then be recovered from $\tilde{\xi}(\mu)$ from the reduced basis map Z :

$$\xi(\mu) \approx Z\tilde{\xi}(\mu), \quad (29)$$

where Z is a suitable matrix with m columns and \mathcal{N} lines (see [31]). The Z matrix will be assumed, without loss of generality, to have unit and orthogonal column vectors, which are the vectors of the reduced basis.

We define the standard Euclidean norm: $\|x\| = \sqrt{x^T x}$. Since the discrete output can be written as

$$f_{\text{discrete}}(\mu) = \|\xi(\mu)\|, \quad (30)$$

the reduced approximation of the output reads:

$$\tilde{f}_{\text{discrete}}(\mu) = \|\tilde{\xi}(\mu)\|. \quad (31)$$

A fully-computable error bound between the solution of the reduced model and the solution of the model is available (op. cit.), which means that the error in (29) can be quantified. This error bound is given in the theorem below:

Theorem 2 [36] *For any μ , we have:*

$$\|\xi(\mu) - Z\tilde{\xi}(\mu)\| \leq \frac{\rho(\mu)}{\alpha(\mu)}, \quad (32)$$

where

$$\rho(\mu) = \|A(\mu)Z\tilde{\xi}(\mu) - b(\mu)\|$$

and $\alpha(\mu)$ is any real number which satisfies:

$$0 < \alpha(\mu) \leq \inf_{v, \|v\|=1} |v^T A(\mu)v|. \quad (33)$$

The papers [36] and [27] give efficient methods to compute $\rho(\mu)$, and an $\alpha(\mu)$ which satisfies (33), respectively.

Corollary 2 *For any μ , we have:*

$$\left| f_{\text{discrete}}(\mu) - \tilde{f}_{\text{discrete}}(\mu) \right| \leq \frac{\rho(\mu)}{\alpha(\mu)},$$

where $\rho(\mu)$ and $\alpha(\mu)$ are as in Theorem 2.

Proof of Corollary 2 The proof follows from the reverse triangle inequality, (30), (31) and (32) in Theorem 2. \square

Remark 2 The bound in Corollary 2 depends on the size m of the reduced basis. Hence, we are in the framework of Section 3.2, where our “true” output is $Y = f_{\text{discrete}}(\mu)$, and where the metamodel output is $\tilde{Y} = \tilde{f}_{\text{discrete},m}(\mu)$. The upper bound for the metamodel error is given by

$$\delta_m(\mu) = \left| f_{\text{discrete}}(\mu) - \tilde{f}_{\text{discrete},m}(\mu) \right| \leq \frac{\rho_m(\mu)}{\alpha(\mu)}.$$

In the numerical experiments, we will calibrate the reduced basis size m with respect to the Monte-Carlo sample size n , in order that $\delta_m(\mu)$ satisfy the assumptions of Corollary 1 as the Monte-Carlo sample size n grows to infinity. Note that the calibration of m does not require the evaluation of the true model f , just of the error bound, for which efficient algorithms are available, see e.g. [36] or [27].

4 Numerical results

4.1 Parameters

In Table 1 below, we fix numerical values for the expectations and variances of the probability distributions modeling the uncertainty of parameters h_s , B , S_b , C , z_{up} , ξ_1^0 , ξ_2^0 , μ_0 and μ_L (see Section 2.3 for more details).

Name	Nominal value	Comment
h_s	$4m$	uncertainty: $\mathcal{N}(4, 0.03)$
B	$80m$	uncertainty $\mathcal{N}(80, 1.03)$
S_b	0.0002	uncertainty $\mathcal{N}(2 \times 10^{-4}, 2.5 \times 10^{-6})$
C	0.001	uncertainty $\mathcal{U}([9 \times 10^{-4}, 0.0011])$
z_{up}	$10m$	uncertainty $\mathcal{N}(10, 0.13)$
ξ_1^0	0	initial value, uncertainty $\mathcal{U}([-0.01, 0.01])$
ξ_2^0	0	initial value, uncertainty $\mathcal{U}([-0.01, 0.01])$
μ_0	0.65	uncertainty $\mathcal{N}(0.65, 0.0066)$
μ_L	0.65	uncertainty $\mathcal{N}(0.65, 0.0066)$
k_0	0.6	known
k_L	0.7	known
Q^*	50	known
g	9.81	acceleration of gravity, known

Table 1 Uncertainty on input parameters. $\mathcal{N}(m, \sigma)$ is a normal distribution of mean value m and standard deviation σ , and $\mathcal{U}([a, b])$ is the uniform distribution on $[a, b]$.

For the numerical implementations, we have chosen the channel length $L = 250m$, and the time horizon $T^* = 75s$. The parameters k_0 and k_L have been fixed to 0.6 and 0.7, satisfying condition (14) for the stability of the nominal closed-loop system. The discretization parameters were set to $\Delta t = 5s$, $\Delta x = 5m$, and for the reduction, a reduced basis obtained from proper orthogonal decomposition [42] of size m (to determine, see the next Subsection), obtained from a snapshot of size 100. For the estimation of Sobol' indices, the Monte-Carlo sample size was fixed equal to $n = 30000$. We provide asymptotic CI of level 0.95.

Note that the length of a CI is a direct measurement of the estimation precision.

4.2 Calibration of m

In this section, we see how to choose the reduced basis size m depending on the Monte-Carlo sample size n , in order to get asymptotic confidence intervals for the sensitivity indices. The idea is to fix m as a function of n so as to satisfy the condition of Corollary 1. We first need to estimate the variance of the error:

$$\delta(\mu, m) = \tilde{f}_m(\mu) - f(\mu)$$

as a function of m . To do so, we compute samples of δ 's:

$$\mathcal{S}_m = \{\delta(\mu, m), \mu \in \Xi\}$$

where Ξ is a random sample of size 1000, and $m = 3, 4, \dots, 14$, and we estimate $\text{Var}\delta(\mu, m)$ by its empirical estimator $\widehat{\text{Var}}\delta(\mu, m)$. The result is given in Figure 4.

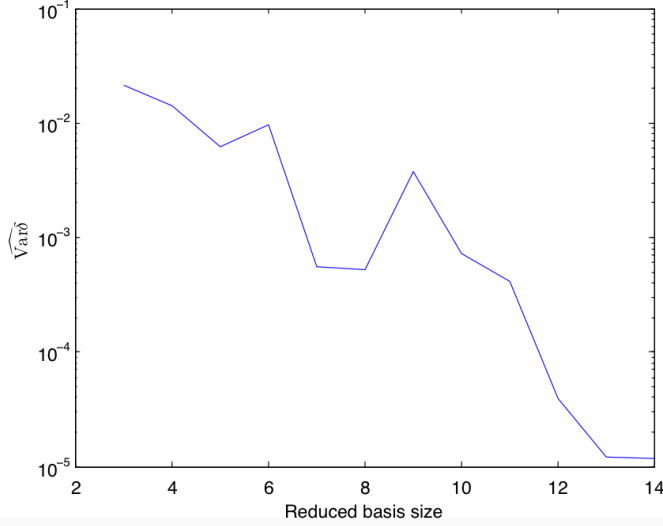


Fig. 4 Plot of $\ln \widehat{\text{Var}}\delta(\mu, m)$ as a function of the reduced basis size m .

The plot suggests a log-linear regression of $\text{Var}\delta(\mu, m)$ as a function of m . We suppose that the following approximation holds:

$$\text{Var} \left(\tilde{f}_{discrete, m}(\mu) - f_{discrete}(\mu) \right) \approx cq^m \quad (34)$$

where $c = 0.2414$, $q = 0.5070$ (obtained by least-square fitting).

Set $m = m(n)$, and $\tilde{f}_n = \tilde{f}_{discrete, m(n)}$. We have, for $n \rightarrow +\infty$:

$$n \text{Var} \left(\tilde{f}_n(\mu) - f_{discrete}(\mu) \right) \rightarrow 0$$

as soon as

$$ncq^{m(n)} \leq 1/\gamma(n),$$

for any γ function such that $\lim_{n \rightarrow +\infty} \gamma(n) = +\infty$, that is to say

$$m(n) \geq -\frac{\log(nc\gamma(n))}{\log q}.$$

To illustrate our asymptotic, we take $n = 30000$, and $\gamma(n) = \log \log(n)$. Hence, we choose m according to:

$$m = m(n) = -\frac{\log(nc \log(\log(n)))}{\log q} \approx 14.$$

4.3 Indices estimations

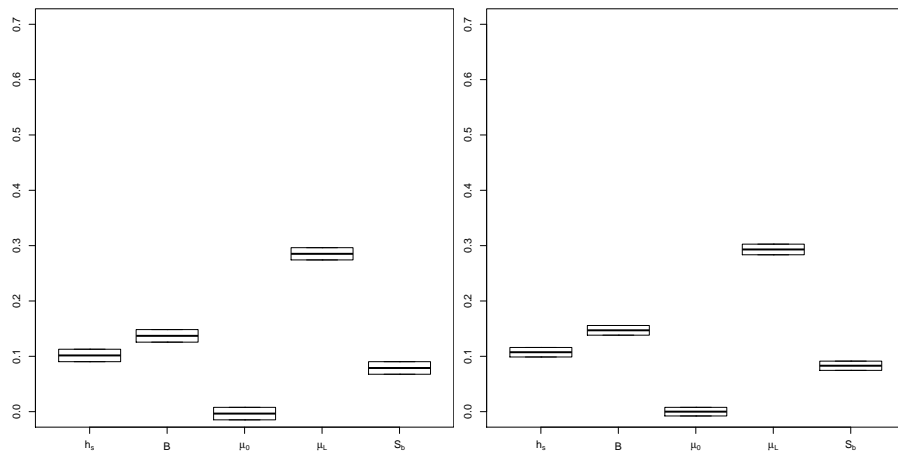


Fig. 5 First-order (left) and total (right) Sobol' indices with 95% CI for for each labelled uncertain parameter: h_s , B , μ_0 , μ_L , S_b (from left to right on the horizontal axis).

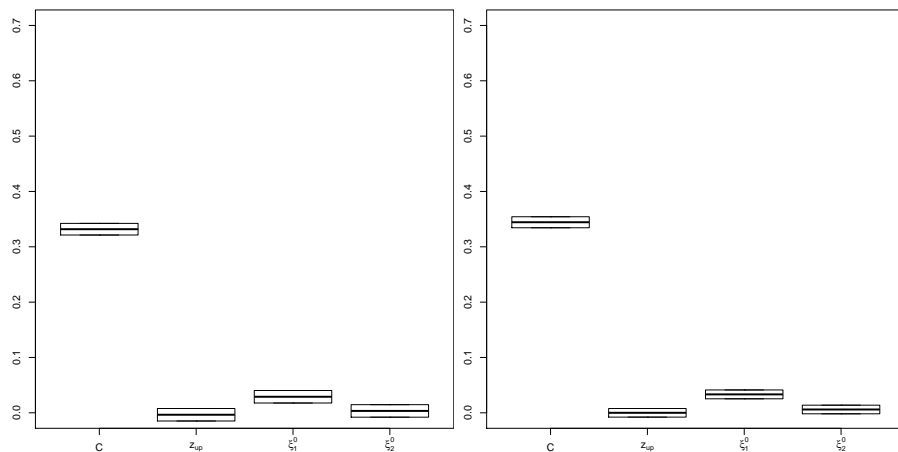


Fig. 6 First-order (left) and total (right) Sobol' indices with 95% CI for for each labelled uncertain parameter: C , z_{up} , ξ_1^0 , and ξ_2^0 (from left to right on the horizontal axis).

On Figures 5 and 6 the results read as follows. For each uncertain parameter, the bold centered line on the left part of the figure (respectively on the right part) gives, on the vertical axis, the estimation of the first-order (resp. total) Sobol' index. The upper and lower thin lines define the upper and lower bounds of the 95% CI. Note that, by definition, the first-order index is smaller than the corresponding total index. We conclude with a confidence level of 95% that the influence of the parameters z_{up} and μ_0 are not significant for this *to-be-controlled output*. As expected from the choice of T^* and the exponential control rate, the initial conditions (ξ_1^0, ξ_2^0) are not significant as well. The parameter C is the parameter having the most significant effect, parameters S_b and B are influent as well but to a less extent.

The influence of μ_L is clearly greater than the influence of μ_0 . Therefore as far as the *to-be-controlled output* is concerned, a precise knowledge on the value of physical parameter μ_L is necessary, in contrast to the knowledge of μ_0 which seems to have a smaller impact on the control objective.

For each parameter, as the difference between the total and the first-order indices is not significant, it means that the interactions are negligible. Thus the *to-be-controlled output* is additive in the parameters.

4.4 Additive modeling of the output

The previous results suggested that the *to-be-controlled output* can be well-approximated by an additive function:

$$f_{discrete} \approx \sum_{x \in \mathcal{V}} g_x \quad (35)$$

where \mathcal{V} is a subset of all the parameters' symbols:

$$\mathcal{V} \subset \mathcal{V}_0 = \{h_s, B, \mu_0, \mu_L, S_b, C, z_{up}, \xi_1^0, \xi_2^0\},$$

and the g_x are appropriate univariate functions, that will be fitted using a random iid. sample of 3000 outputs.

There are two possible choices for \mathcal{V} : the "full" choice $\mathcal{V} = \mathcal{V}_0$, and the "reduced" choice:

$$\mathcal{V} = \mathcal{V}_0 \setminus \{\mu_0, z_{up}, \xi_2^0\}$$

consisting of all the parameters detected as the most influent by our sensitivity analysis.

The g_x functions can be chosen, either as linear functions (leading to linear regression) or splines (leading to generalized additive modeling (GAM) by splines).

These two-by-two possible choices hence give rise to four possible models. The Akaike information criterion (AIC) is used to compare these four models and select the best one. AIC indeed deals with the trade-off between the goodness of fit of the model and its complexity, see [1]. The computations have

Model	AIC
Full + Linear	-9938
Full + Spline	-10837
Reduced + Linear	-9536
Reduced + Spline	-10319

Table 2 Fitted Akaike information criterions for the different considered models. The smaller the AIC, the better the model, in terms of bias/variance compromise.

been made by using the packages `gam` [23] and `stats` [38] packages of the R statistical software [38]. The computed AICs are reported in Table 2.

Table 2 shows the superiority of the GAM (spline) model, compared with the simple linear model. However, using the full set of variables also gives a better AIC than using the reduced one. We hence try:

$$\mathcal{V} = \mathcal{V}_0 \setminus \{\mu_0, z_{up}\}, \quad (36)$$

as ξ_2^0 is the “least negligible” parameter pointed out by sensitivity analysis. The reported AIC for this choice of \mathcal{V} is -10847, which is the best AIC obtained. Hence we decide to retain GAM and (36) to model $f_{discrete}$.

The fitted functions g_x are gathered in Figure 7. We see that all the parameters have a monotonic effect on the output (increasing for h_s , B , μ_L , decreasing for the other), and also that all the effects are very close to linear, except for the B parameter, which has a significantly nonlinear (convex) effect.

5 Conclusion

In this paper, the global sensitivity analysis has been performed when considering probabilistic distribution functions standing for the uncertainty in some unknown physical parameters. It allows us to describe the impact of the parameters on a *to-be-controlled output* in a boundary control problem. This boundary control is motivated by an application for the flow control in an open channel where water height and velocity are described by the Shallow Water equations, in presence of friction and bottom slopes. The *to-be-controlled output* has been defined as the norm of the state at a given large time. We deduce from the numerical studies that some parameters have a nonlinear effect (such as B) whereas other parameters have a linear effect, such as the parameter C appearing in the friction slope S_f , which is usually not well modeled in the literature. Concerning the physical parameters μ_0 and μ_L , it appears that a precise knowledge of μ_L is more important than the knowledge of μ_0 (since the latter parameter is less influent on the *to-be-controlled output*).

This work lets many research lines open. In particular, it could be interesting to optimize the control parameters k_0 and k_L by adding them in the global sensitivity analysis. Another open question is to provide the *a posteriori* error estimator for the reduced basis approach with a nonlinear output. This latter study is currently under investigation.

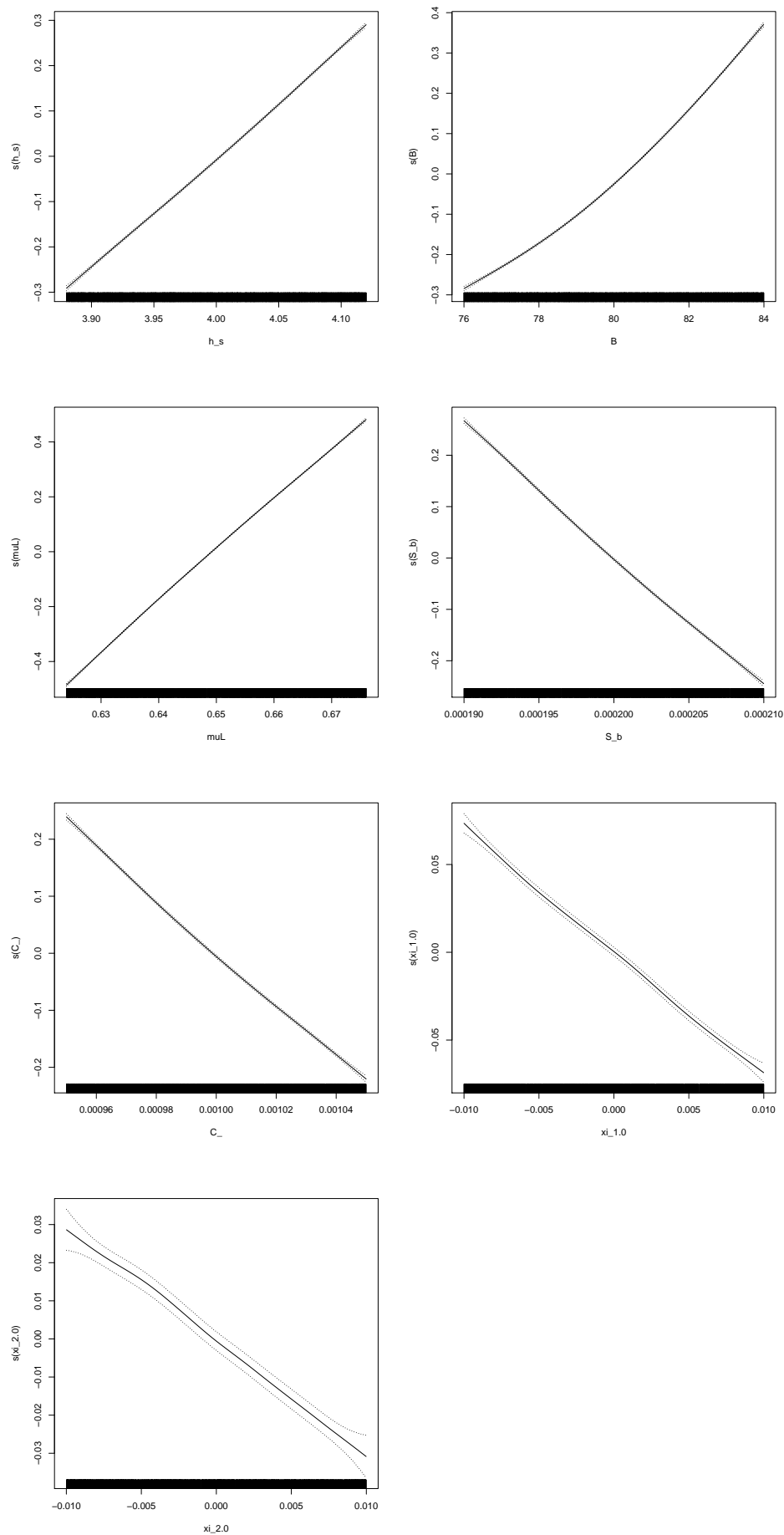


Fig. 7 The fitted g_x spline functions in (35), for $x \in \mathcal{V}$ defined by (36): h_s , B , μ_L , S_b , C , ξ_1^0 , and ξ_2^0 (from top left to down, line by line). The dotted lines are the 95% confidence bands.

A Technical proofs

A.1 Proof of Proposition 1

Proof of Proposition 1. Let us first note that it follows from (2) and $Q = BHV$ that (by omitting the time variable)

$$BH(0)V(0) = U_0 B \mu_0 \sqrt{2g(z_{up} - H(0))}$$

which is equivalent to

$$V(0) = U_0 \frac{1}{H(0)} \mu_0 \sqrt{2g(z_{up} - H(0))}. \quad (37)$$

On the other side the first line of (13) yields with (7) and the definitions of v and h , the following

$$\begin{aligned} V(0) - V^* + (H(0) - H^*) \sqrt{\frac{g}{H^*}} \\ = k_0(V(0) - V^*) - k_0(H(0) - H^*) \sqrt{\frac{g}{H^*}}, \end{aligned}$$

which may be rewritten as

$$V(0) = V^* - \frac{1 + k_0}{1 - k_0} (H(0) - H^*) \sqrt{\frac{g}{H^*}}. \quad (38)$$

Therefore, with (37) and (38), (2) and the first line of (13) are equivalent as soon as the first control is defined by (11).

Let us compute the control U_L in a similar way. To do that, we first deduce from (3) the following

$$(H(L) - h_s - U_L)^3 = \frac{H(L)^2 V(L)^2}{2g\mu_L^2}$$

and thus

$$V(L) = \frac{\sqrt{2g\mu_L^2 (H(L) - h_s - U_L)^3}}{H(L)} \quad (39)$$

Moreover from the second line of (13), with (7) and the expressions of v and h , it holds

$$\begin{aligned} V(L) - V^* - (H(L) - H^*) \sqrt{\frac{g}{H^*}} \\ = k_L(V(L) - V^*) + k_L(H(L) - H^*) \sqrt{\frac{g}{H^*}} \end{aligned}$$

and also

$$V(L) = V^* + \frac{1 + k_L}{1 - k_L} (H(L) - H^*) \sqrt{\frac{g}{H^*}} \quad (40)$$

From (39) and (40) we get that (3) and the second line (13) are equivalent as soon as the control U_L is defined by

$$\begin{aligned} \sqrt{2g\mu_L^2 (H(L) - h_s - U_L)^3} \\ = H(L) \left(V^* + \frac{1 + k_L}{1 - k_L} (H(L) - H^*) \sqrt{\frac{g}{H^*}} \right) \end{aligned}$$

which is equivalent to (12). This concludes the proof of Proposition 1. \square

A.2 Proof of Proposition 3

Proof of Proposition 3. For sake of conciseness, we omit the time variable: for instance $H(0)$ stands for $H(0, t)$ for each t . Let us define $\alpha = \frac{1+k_0}{1-k_0}$, $\beta = \sqrt{\frac{g}{H_{\text{nom}}^*}}$.

At $x = 0$, we take, from the proof of Proposition 1:

$$H(0)V(0) = U_0\mu_0\sqrt{2g(z_{up} - H(0))}$$

with

$$U_0 = \frac{H(0)(V_{\text{nom}}^* - \alpha(H(0) - H_{\text{nom}}^*)\beta)}{\mu_0\sqrt{2g(z_{up, \text{nom}} - H(0))}}$$

that is:

$$v(0) = \sqrt{\frac{z_{up} - H(0)}{z_{up, \text{nom}} - H(0)}} (V_{\text{nom}}^* - \alpha(H(0) - H_{\text{nom}}^*)\beta) - V^*.$$

Now, given the change of variables between (V, H) , (v, h) , this equation could be rewritten as a nonlinear relation between $v(0)$ and $h(0)$, hence, as a nonlinear relation between $\xi_1(0)$ and $\xi_2(0)$. However, to keep the resolution simple, we have to linearize this equation. This linearization is made in accordance with the linearization of the Shallow-Water equation for (H, V) near (H^*, V^*) , hence for (h, v) near the origin. We do the same here; hence by Taylor expansion around $h = 0$, we get $v(0) = \mathcal{A} + \mathcal{B}h(0) + o(h(0))$ with

$$\mathcal{A} = \frac{\mu_0}{\mu_{0, \text{nom}}} \sqrt{\frac{H^* - z_{up}}{H^* - z_{up, \text{nom}}}} (V_{\text{nom}}^* - \alpha\beta(H^* - H_{\text{nom}}^*)) - V^*,$$

and

$$\mathcal{B} = \frac{\mu_0}{\mu_{0, \text{nom}}} \sqrt{\frac{H^* - z_{up}}{H^* - z_{up, \text{nom}}}} \left(-\alpha\beta + \frac{(z_{up} - z_{up, \text{nom}})(V_{\text{nom}}^* - \alpha\beta(H^* - H_{\text{nom}}^*))}{2(H^* - z_{up})(H^* - z_{up, \text{nom}})} \right).$$

Similarly, at $x = L$, we have

$$V(L) = \frac{\sqrt{2g}\mu_L}{H(L)} \left(e_h + \left(\frac{H(L)(V_{\text{nom}}^* + \alpha_L\beta e_H)}{\sqrt{2g}\mu_L} \right)^{2/3} \right)^{3/2}$$

where $\alpha_L = \frac{1+k_L}{1-k_L}$, and

$$e_h = h_{s, \text{nom}} - h_s, \quad e_H = H(L) - H_{\text{nom}}^*.$$

Therefore,

$$v(L) = \mathcal{C} + \mathcal{D}h(L) + o(h(L)),$$

with

$$\begin{aligned} \mathcal{C} &= \frac{\sqrt{2g}}{4} \mu_L (2h_{s, \text{nom}} - 2h_s \\ &\quad + 2^{2/3} \left(-H^* \frac{(-V_{\text{nom}}^* + \alpha_L\beta_{\text{nom}} H_{\text{nom}}^*)}{(\sqrt{g}\mu_{L, \text{nom}})} \right)^{2/3}) \\ &\quad \sqrt{\frac{\left(4h_{s, \text{nom}} - 4h_s + 2 \times 2^{2/3} \left(-H^* \times \frac{(-V_{\text{nom}}^* + \alpha_L\beta_{\text{nom}} H_{\text{nom}}^*)}{(\sqrt{g}\mu_{L, \text{nom}})} \right)^{2/3} \right)}{H^*}} \\ \mathcal{D} &= -\frac{1}{2} \left(2^{1/6} \left(-H^* \frac{(-V_{\text{nom}}^* + \alpha_L\beta_{\text{nom}} H_{\text{nom}}^*)}{(\sqrt{g}\mu_{L, \text{nom}})} \right)^{2/3} \alpha_L\beta_{\text{nom}} H^* \right. \\ &\quad - \sqrt{2}V_{\text{nom}}^* h_{s, \text{nom}} + \sqrt{2}V_{\text{nom}}^* h_s + \sqrt{2}\alpha_L\beta_{\text{nom}} H_{\text{nom}}^* h_{s, \text{nom}} \\ &\quad \left. - \sqrt{2}\alpha_L\beta_{\text{nom}} H_{\text{nom}}^* h_s \right) \\ &\quad \sqrt{\frac{\left(4h_{s, \text{nom}} - 4h_s + 2 \times 2^{2/3} \left(-H^* \frac{(-V_{\text{nom}}^* + \alpha_L\beta_{\text{nom}} H_{\text{nom}}^*)}{(\sqrt{g}\mu_{L, \text{nom}})} \right)^{2/3} \right)}{\mu_L \frac{\sqrt{g}}{((-V_{\text{nom}}^* + \alpha_L\beta_{\text{nom}} H_{\text{nom}}^*)H^{*2})}}} \end{aligned}$$

Thus, the linearized boundary relations satisfied by ξ_1 and ξ_2 in the real-life model are given by (18) and (19). \square

References

1. H. Akaike. A new look at the statistical model identification. *IEEE Transactions on Automatic Control*, 19(6):716–723, 1974.
2. F. Alabau-Boussouira. Insensitizing exact controls for the scalar wave equation and exact controllability of 2-coupled cascade systems of PDE’s by a single control. *Mathematics of Control, Signals, and Systems*, 26(1):1–46, 2014.
3. G. Bastin, J.-M. Coron, and B. d’Andréa Novel. Using hyperbolic systems of balance laws for modeling, control and stability analysis of physical networks. In *Lecture notes for the Pre-Congress Workshop on Complex Embedded and Networked Control Systems*, Seoul, Korea, 2008. 17th IFAC World Congress.
4. G. Bastin, J.-M. Coron, and B. d’Andréa Novel. On Lyapunov stability of linearised Saint-Venant equations for a sloping channel. *Networks and Heterogeneous Media*, 4(2):177–187, 2009.
5. O. Bodart and C. Fabre. Controls insensitizing the norm of the solution of a semilinear heat equation in unbounded domains. *J. Math. Anal. and App.*, 195:658–683, 1995.
6. O. Bodart, M. González-Burgos, and R. Pérez-García. Existence of insensitizing controls for a semilinear heat equation with a superlinear nonlinearity. *Communications in Partial Differential Equations*, 29(7-8):1017–1050, 2004.
7. J.-M. Coron. *Control and Nonlinearity*, volume 136 of *Mathematical Surveys and Monographs*. American Mathematical Society, Providence, RI, 2007.
8. J.-M. Coron, G. Bastin, and B. d’Andréa Novel. Dissipative boundary conditions for one-dimensional nonlinear hyperbolic systems. *SIAM Journal on Control and Optimization*, 47(3):1460–1498, 2008.
9. R.I. Cukier, H.B. Levine, and K.E. Shuler. Nonlinear sensitivity analysis of multiparameter model systems. *Journal of computational physics*, 26(1):1–42, 1978.
10. R. Dáger. Insensitizing controls for the 1-D wave equation. *SIAM Journal on Control and Optimization*, 45(5):1758–1768, 2006.
11. L. de Teresa. Controls insensitizing the norm of the solution of a semilinear heat equation in unbounded domains. *ESAIM: Control, Optimisation and Calculus of Variations*, 2:125–149, 1997.
12. L. de Teresa. Insensitizing controls for a semilinear heat equation. *Communications in Partial Differential Equations*, 25(1-2):39–72, 2000.
13. L. de Teresa and E. Zuazua. Identification of the class of initial data for the insensitizing control of the heat equation. *Commun. Pure Appl. Anal*, 8(1):457–471, 2009.
14. V. Dos Santos and C. Prieur. Boundary control of open channels with numerical and experimental validations. *IEEE Transactions on Control Systems Technology*, 16(6):1252–1264, 2008.
15. B. Efron and C. Stein. The jackknife estimate of variance. *The Annals of Statistics*, 9(3):586–596, 1981.
16. K.-T. Fang, R. Li, and A. Sudjianto. *Design and modeling for computer experiments*. CRC Press, 2005.
17. E. Fernández-Cara, G.C. Garcia, and A. Osses. Insensitizing controls for a large-scale ocean circulation model. *Comptes Rendus Mathématique*, 337(4):265–270, 2003.
18. F. Gamboa, A. Janon, T. Klein, A. Lagnoux-Renaudie, and C. Prieur. Statistical inference for Sobol pick freeze Monte Carlo method. *Statistics*, to appear, 2016.
19. M.A. Grepl, Y. Maday, N.C. Nguyen, and A.T. Patera. Efficient reduced-basis treatment of nonaffine and nonlinear partial differential equations. *Mathematical Modelling and Numerical Analysis*, 41(3):575–605, 2007.
20. M.A. Grepl and A.T. Patera. A posteriori error bounds for reduced-basis approximations of parametrized parabolic partial differential equations. *Mathematical Modelling and Numerical Analysis*, 39(1):157–181, 2005.

21. S. Guerrero. Controllability of systems of stokes equations with one control force: existence of insensitizing controls. *Annales de l'Institut Henri Poincaré (C) Non Linear Analysis*, 24(6):1029–1054, 2007.
22. M. Gueye. Insensitizing controls for the navier–stokes equations. *Annales de l'Institut Henri Poincaré (C) Non Linear Analysis*, 30(5):825–844, 2013.
23. T. Hastie. *gam: Generalized Additive Models*, 2014. R package version 1.09.1.
24. J.C. Helton, J.D. Johnson, C.J. Sallaberry, and C.B. Storlie. Survey of sampling-based methods for uncertainty and sensitivity analysis. *Reliability Engineering & System Safety*, 91(10-11):1175–1209, 2006.
25. W. F. Hoeffding. A class of statistics with asymptotically normal distributions. *Annals of Mathematical Statistics*, 19:293–325, 1948.
26. T. Homma and A. Saltelli. Importance measures in global sensitivity analysis of non-linear models. *Reliability Engineering & System Safety*, 52(1):1–17, 1996.
27. D.B.P. Huynh, G. Rozza, S. Sen, and A.T. Patera. A successive constraint linear optimization method for lower bounds of parametric coercivity and inf-sup stability constants. *Comptes Rendus Mathématique*, 345(8):473–478, 2007.
28. A. Janon, T. Klein, A. Lagnoux, M. Nodet, and C. Prieur. Asymptotic normality and efficiency of two Sobol index estimators. *ESAIM: Probability and Statistics*, 18:342–364, 2014.
29. A. Janon, M. Nodet, and C. Prieur. Certified reduced-basis solutions of viscous Burgers equation parametrized by initial and boundary values. *ESAIM: Mathematical Modelling and Numerical Analysis*, 47(2):317–348, March 2013.
30. A. Janon, M. Nodet, and C. Prieur. Uncertainties assessment in global sensitivity indices estimation from metamodels. *International Journal for Uncertainty Quantification*, 4(1):21–36, 2014.
31. A. Janon, M. Nodet, and C. Prieur. Goal-oriented error estimation for reduced basis method, with application to certified sensitivity analysis. *Journal of Scientific Computing*, to appear, 2015.
32. A. Janon, M. Nodet, Ch. Prieur, and Cl. Prieur. Global sensitivity analysis for the boundary control of an open channel. In *53rd IEEE Conference on Decision and Control*, pages 589–594, Los Angeles, United States, December 2014.
33. T.-T. Li. *Global classical solutions for quasilinear hyperbolic systems*, volume 32 of *RAM: Research in Applied Mathematics*. Masson, Paris, 1994.
34. S. Micu, J.H. Ortega, and L. de Teresa. An example of ϵ -insensitizing controls for the heat equation with no intersecting observation and control regions. *Applied Mathematics Letters*, 17(8):927–932, 2004.
35. H. Monod, C. Naud, and D. Makowski. Uncertainty and sensitivity analysis for crop models. In D. Wallach, D. Makowski, and J.W. Jones, editors, *Working with Dynamic Crop Models: Evaluation, Analysis, Parameterization, and Applications*, chapter 4, pages 55–99. Elsevier, 2006.
36. N.C. Nguyen, K. Veroy, and A.T. Patera. Certified real-time solution of parametrized partial differential equations. *Handbook of Materials Modeling*, pages 1523–1558, 2005.
37. C. Prieur, J. Winikin, and G. Bastin. Robust boundary control of systems of conservation laws. *Mathematics of Control, Signals, and Systems*, 20(2):173–197, 2008.
38. R Core Team. *R: A Language and Environment for Statistical Computing*. R Foundation for Statistical Computing, Vienna, Austria, 2014.
39. A. Saltelli, K. Chan, and E.M. Scott. *Sensitivity analysis*. Wiley Series in Probability and Statistics. John Wiley & Sons, Ltd., Chichester, 2000.
40. T. J. Santner, B. Williams, and W. Notz. *The Design and Analysis of Computer Experiments*. Springer-Verlag, 2003.
41. R. Schaback. Mathematical results concerning kernel techniques. In *Prep. 13th IFAC Symposium on System Identification, Rotterdam*, pages 1814–1819. Citeseer, 2003.
42. L. Sirovich. Turbulence and the dynamics of coherent structures. Part I-II. *Quarterly of applied mathematics*, 45(3):561–590, 1987.
43. I.M. Sobol'. Sensitivity analysis for nonlinear mathematical models. *Mathematical Modeling and Computational Experiment*, 1:407–414, 1993.
44. I.M. Sobol'. Global sensitivity indices for nonlinear mathematical models and their Monte Carlo estimates. *Mathematics and Computers in Simulation*, 55(1-3):271–280, 2001.

45. B. Sudret. Global sensitivity analysis using polynomial chaos expansions. *Reliability Engineering & System Safety*, 93(7):964–979, 2008.
46. J.-Y. Tissot and C. Prieur. A randomized orthogonal array-based procedure for the estimation of first- and second-order Sobol’ indices. *Journal of Statistical Computation and Simulation*, 85(7):1358–1381, 2015.
47. K. Veroy and A.T. Patera. Certified real-time solution of the parametrized steady incompressible Navier-Stokes equations: Rigorous reduced-basis a posteriori error bounds. *International Journal for Numerical Methods in Fluids*, 47(8-9):773–788, 2005.